

FEDSM2021-61460

DUAL-LUMINESCENCE IMAGING AND PARTICLE TRACKING VELOCIMETRY FOR SIMULTANEOUS TEMPERATURE AND VELOCITY FIELD MEASUREMENTS IN HYDROCARBONS LIQUID

Tatsunori Hayashi¹, Hamed F. Farahani², Ali S. Rangwala², Hirotaka Sakaue¹

¹ Department of Aerospace and Mechanical Engineering, University of Notre Dame, Notre Dame, IN

² Fire Protection Engineering, Worcester Polytechnic Institute, 50 Prescott Street (Gateway Park II)
Worcester, MA

ABSTRACT

Arctic oil spills are particularly detrimental as they could cause extensive ice melting in addition to the environmental pollution they create. Floating oil slicks amongst ice floes absorb ambient energy and transfer that energy to the ice to aggravate melting in the thaw season. However, few studies have been undertaken to reveal how oil-ice interactions impact ice melting. This research employs a measurement technique to investigate the heat transfer pathways from oil slicks to the ice. Dual-luminescence imaging and particle imaging velocimetry (PIV) in a side cooled cavity is performed for temperature and velocity measurements of Toluene, respectively. Dual-luminescence imaging captured the spatial temperature distribution of the fuel. Consecutive imaging of the seeding particles in PIV provided the spatial velocity field of the fuel in the cavity. The results show that the convective field is directly coupled with the temperature field, i.e., the temperature difference instigates a flow in the liquid. Successful implementation of the two measuring techniques together is a step toward analyzing heat transfer pathways in a liquid fuel adjacent to an ice body, indicating the extent of melting.

Keywords: Luminescence technique, dual-luminescence imaging, particle-based velocimetry, simultaneous temperature, and velocity field measurement

A, B Coefficients from first-order polynomial
 σ_T Temperature sensitivity
Subscripts
 ij Pixel location of camera output

1. INTRODUCTION

Tons of oil or chemicals are accidentally released into the environment each year [1]. Accidents around coastal areas can harm the environment and have a negative impact on nature. Arctic oil spills are particularly detrimental as they could potentially cause extensive ice melting in addition to the environmental pollution they create [2]. A large-scale spill in the Arctic waters, similar to the Deepwater Horizon spill in 2012, could trigger ice sheet deterioration and negatively impact climate cycles globally [3]. Floating oil slicks amongst ice floes absorb ambient energy, i.e., sunlight or energy sources created by cleanup operations such as in situ burning and transfer that energy to the ice to aggravate melting in the thaw season. However, only a few studies have been undertaken to reveal how oil-ice interaction impacts ice melting [4–6]. In particular, melting caused by an adjacent immiscible liquid layer and heat transfer to ice in such a condition is not well understood, and basic temperature and velocity field measurements are required to understand the heat transfer mechanisms of an immiscible layer. This research employs a newly developed simultaneous temperature and velocity field measurement technique to investigate the coupling between temperature and velocity field of a fuel layer cooled on the side. A two-dimensional temperature measurement of the fuel is performed by developing dual-luminescence imaging [7]. The two luminescent probes used in dual-luminescence imaging have different fluorescent characteristics: one of the two luminescent probes emits a temperature-dependent luminescence, another probe outputs temperature-independent luminescence. The luminescent peaks

NOMENCLATURE

V_R Red image output of a camera
 V_B Blue image output of a camera
 G Geometric factor
 I_{Eu} Luminescent intensity of $\text{Eu}(\text{hfc})_3$
 I_{PC} Luminescent intensity of PCA
 N Camera shot noise
 T Temperature
 S Intensity ratio

of the two probes should lie at different wavelengths so that each luminescent output can be acquired by different color images using a high-speed color camera. By taking the ratio of the different color images, spatiotemporal temperature information of the liquid fuel can be extracted [8]. One challenge in terms of the luminescent technique is the dynamic motion of ice as it is melting. The ice-melting moves the geometric position of the ice, especially the interface between the ice and the oil. Because of this dynamic motion, dual-luminescence imaging, which is able to capture temperature information over moving objects, is chosen as a unique diagnostic tool. However, the focus of the current study is the development of this technique for a liquid fuel layer without the presence of ice. Determining the two luminescent probes used to measure the spatiotemporal temperature of the fuel is one of the essential requirements for establishing this luminescent imaging technique. Toluene is selected to represent the spilled oil, which is immiscible in water as most hydrocarbon petroleum fuels are. Europium-based and Pyrene-based luminescent probes are dissolved into Toluene to create the dual-luminescence oil. Colored-seeding particles were mixed into pure Toluene to capture the velocity field of the liquid phase via a particle-based velocimetry technique. A combination of the two measurements for dual-luminescence oil in a side cooled cavity was performed to capture both temperature and velocity field information. In this research, the temperature measurement and velocity field measurement were conducted separately as the first step. In future works, simultaneous temperature and velocity field measurements of an immiscible layer adjacent to ice will be conducted. The side cooled cavity used here, simply imitates the ice-oil interface except for the ice melting, which will be added to future experiments. The current results show that the convective field is directly coupled with the temperature field, i.e., the temperature difference instigates a flow in the oil. Successful implementation of the two measurement techniques together is a step toward analyzing heat transfer pathways in a liquid fuel adjacent to an ice body, providing insight into the extent of the melting.

2. BACKGROUND

2.1 Dual-Luminescence Imaging

Dual-luminescence imaging is a luminescent technique for temperature measurement. The experimental setup of dual-luminescence imaging consists of an excitation light source, dual-luminescence liquid, and a color camera. Dual-luminescence liquid absorbs excitation energy from the light source and emits two different emissions. The color camera captures the fluorescent emissions from the dual-luminescence liquid as luminescent outputs. Consider the luminescent outputs from an arbitrary pixel, ij , on an image chip of the color camera, where the image chip has m by n pixels ($i = 1, 2, \dots, m$, and $j = 1, 2, \dots, n$). At this pixel, the outputs from the blue image, V_{Bij} , and the red image, V_{Rij} , can be described as:

$$V_{Rij} = G_{ij} \times I_{Eu ij}(T) + N_{ij} \quad (1.a)$$

$$V_{Bij} = G_{ij} \times I_{PC ij} + N_{ij} \quad (1.b)$$

where I_{Eu} and I_{PC} are the luminescent outputs from europium tris [3-heptafluoropropylhydroxymethylene-camphorate] ($\text{Eu}(\text{hfc})_3$), and 1-pyrenecarboxylic acid (PCA), respectively. Because $\text{Eu}(\text{hfc})_3$ is a temperature-sensitive luminescent probe, I_{Eu} is temperature-dependent [9]. This is indicated by the functional notation (T) , in Equation 1-a. N indicates the camera shot noise at the pixel ij . The noise factor can be obtained by collecting dark images or images without illumination. By taking an average of multiple noise images, the mean of the shot noise can be obtained. Here, G_{ij} is the geometric factor, which is a function of the pixel location. It is related to the shape and location of a liquid in an image frame, the non-uniformity of the illumination source, and the distance of the liquid and camera. Because the shape and location of a liquid can be changed during the measurement, the three factors above will be time-dependent. To remove G_{ij} from Equation 1, the luminescent ratio shown in Equation 2 was taken.

$$S_{ij} = (V_{Rij} - \overline{N_{ij}}) / (V_{Bij} - \overline{N_{ij}}) = I_{Eu ij}(T) / I_{PC ij} \quad (2)$$

Equation 2 cancels the geometric factor and gives the temperature-dependent output [7]. The function S can be obtained by dividing the red by the blue images after subtracting the mean shot noise. Therefore, the temperature distribution is obtained through an image that is expressed by S . At a pixel where $I_{Eu ij}$ and $I_{PC ij}$ are zero or low signal, the ratio of the two showing Equation 2 would give plus or minus infinity. To avoid this processing error, a threshold can be assigned. For instance, if $I_{Eu ij}$ or $I_{PC ij}$ is lower than the mean shot noise, the ratio, S_{ij} , is assigned zero value.

The intensity ratio monotonically decreases with temperature rise. The relationship between the intensity ratio and temperature, T , can be expressed by the 1st order polynomial:

$$S = A + B \times T \quad (3)$$

where A and B are coefficients of the 1st order polynomial. These coefficients can be determined by experimental temperature calibration. The coefficient, B , is defined as the temperature sensitivity, σ_T :

$$\sigma_T = B \quad (4)$$

In this research, the temperature sensitivity of dual-luminescent oil is calculated using *in-situ* calibration based on the measured temperature by thermocouples.

2.2 Particle-based velocimetry

Particle image velocimetry (PIV) is a common technique for non-intrusive, quantitative, and qualitative flow visualization. In PIV, a thin sheet of light illuminates fluid containing reflective and neutrally buoyant seeding particles. The illuminated seeding particle visualizes a motion of the fluid, either gaseous or liquid. A digital image sensor, which is positioned parallel to the sheet of light, captures the motion of the particles. Two consecutive images of the illuminated plane are captured in most PIV. Particle displacement between consecutive images provides velocities in the sheet. In PIV calculation, the particle displacement for groups of particles allows evaluation of the cross-correlation of many small sub-images based on

interrogation areas. This correlation evaluation yields the most probable displacement for a group of particles displacement.

3. Simultaneous Temperature and Velocity Field Measurement

3.1 Dual-Luminescence Oil

Dual-luminescence oil consists of an organic solvent and two luminescent probes. The organic solvent imitates the liquid fuel under an ice-melting environment. Two luminescent probes for dual-luminescence imaging were dissolved into the solvent. One of the two luminescent probes provides a temperature-dependent luminescent output. The other luminescent probe is independent of the temperature. Two luminescent probes have luminescent outputs that can be separated from each other in terms of a wavelength to detect by the color camera's channels. The resultant combination of the luminescent probes and the solvent as a dual-luminescence oil is $\text{Eu}(\text{hfc})_3$, PCA, and Toluene. The organic solvent mimicking the fuel of liquid hydro carbonate was selected as Toluene. For the temperature-insensitive luminescent probe, PCA was selected because this luminescent probe has less temperature sensitivity than $\text{Eu}(\text{hfc})_3$.

A spectrometer performed spectral measurement with a thermal stage, which controls stage temperature to characterize the dual-luminescent oil. Figure 1 shows the spectra of the dual-luminescence oil. Two luminescent peaks exist at 400 and 610 nm. The peak at a shorter wavelength, which was obtained from PCA, was temperature insensitive. On the contrary, the peak at a higher wavelength obtained from $\text{Eu}(\text{hfc})_3$ was temperature sensitive due to the thermal quenching [2]. Both peaks were matched with the blue and red images of the camera.

The temperature calibration was conducted to characterize the temperature sensitivity of the developed dual-luminescence oil. The temperature varied from 0 to 20 degrees Celsius for the calibration. Figure 2 shows the temperature calibration plot of the dual-luminescence oil. The calculated temperature sensitivities of dual-luminescence oil was -0.4 [%/C]. Here, the temperature sensitivity is defined as a slope of the temperature calibration, and the steeper slope gives a higher temperature-sensitive image.

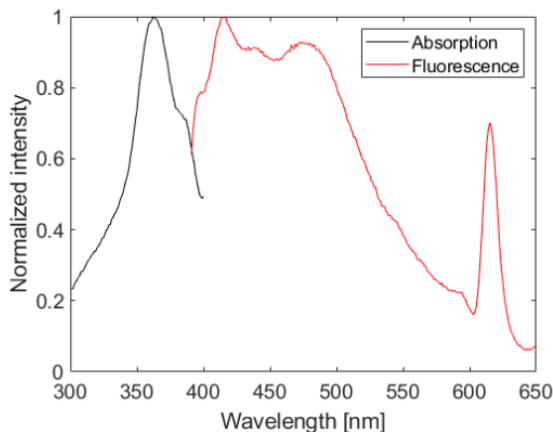


FIGURE 1: ABSORPTION AND EMISSION SPECTRA OF DUAL-LUMINESCENCE OIL.

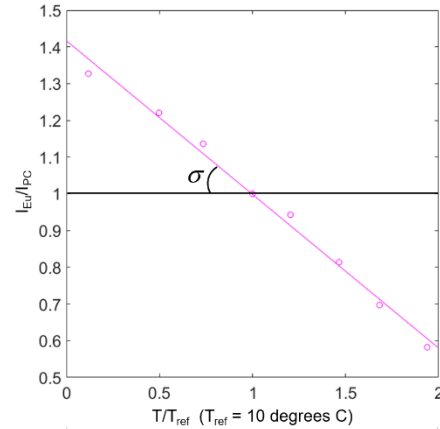


FIGURE 2: TEMPERATURE CALIBRATION PLOT OF DUAL-LUMINESCENCE OIL BETWEEN TEMPERATURE RANGE OF 0 – 20 DEGREE CELSIUS.

3.2 Colored seeding particles

Hollow glass microspheres were mixed into dual-luminescence oil as colored-seeding particles. The mean diameter of the seeding particles varies from 5 - 20 μm . The density of the seeding particles is 0.67 g/cc. Fluorescein was used to color the particles to give particles luminescent output [10–12]. Fluorescein was dissolved into dichloromethane. The concentration of the solution is 1 mM. Seeding particles were soaked in the solution. Then, dichloromethane was evaporated to prepare the colored-seeding particles. The colored seeding particle was mixed into pure Toluene with 1 mg/cc concentration.

3.3 Measurement system

For the development of simultaneous temperature and velocity field measurement, the side cooled cavity was selected. In the side-cooled cavity, natural convection due to the temperature difference between the cool side and other sides induced the velocity field and temperature distribution. This experiment setup imitated the ice-oil interface in which ice cooled the adjacent oil a Peltier cooler was used to mimic low temperatures of an ice surface. A rectangle quartz cuvette contains dual-luminescence oil. The dimension of this cavity was 45 x 50 x 10 mm. All equipment for this experiment were placed in an environmental chamber that could control the temperature. The environmental chamber maintained the ambient temperature surrounding the experimental setup at 20 degrees Celsius. Peltier cooler was set to 0 degrees Celsius and was attached to one side of the cuvette. The other sides were exposed by the ambient temperature. The experiment setup of dual-luminescence imaging is shown in figure 3. Consecutive images were acquired to obtain temporal information over the side-cooled cavity during the experiment. Seeding particles for particle-based velocimetry were mixed into the pure Toluene, and the particles' consecutive imaging provided the spatial velocity field of the oil in the cavity.

The temperature distribution was obtained by dual-luminescence imaging. The optimum concentrations of the two luminescent probes were obtained based on the adjustment of the intensity levels from the two luminescent probes. This procedure gave the two luminescent outputs from each probe similar in the intensity level, and the temperature sensitivity of the two intensities' ratio was high enough for the spatiotemporal imaging. For the excitation light source, two UV-LED light sources excited the dual-luminescence oil at 365 nm. The slits width of this excitation was 2 mm. A high-speed color camera captured a time series of images during temperature measurement. An optical long-pass filter was placed on the optical path of the camera to cut off the wavelength shorter than 420 nm. The frame rate was 100 Hz. The equilibrium condition of natural convection in the cuvette was achieved by waiting for 1 hour. A 1-sec period after this one hour time was recorded and processed to obtain the results. Three thermocouples monitor the temperature in the dual-luminescence oil. For in-situ temperature calibration of dual-luminescence oil, those thermocouples are used.

The velocity field was obtained by the PIV measurement using colored seeing particles. The experimental setup is shown in figure 4, which is very similar to the temperature measurement except for the dual-luminescent oil. Instead of dual-luminescent oil, pure Toluene with colored seeding particles was used. Three thermocouples monitored the temperature of the Toluene. During the recording, thermocouples were removed to reduce the disturbance of the flow.

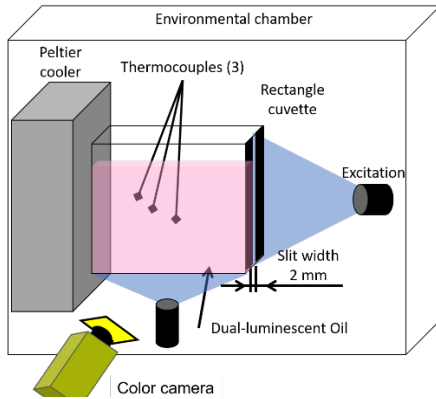


FIGURE 3: EXPERIMENTAL SETUP OF THE SIDE COOLED CAVITY OF DUAL-LUMINESCENCE IMAGING

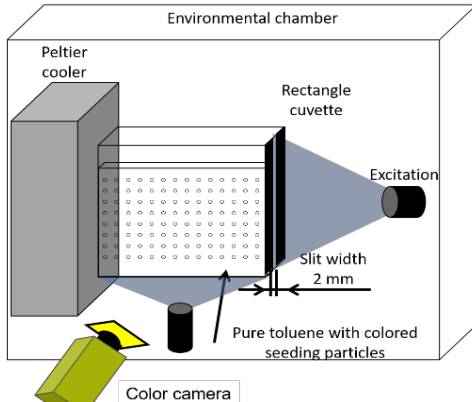


FIGURE 4: EXPERIMENT SETUP OF THE SIDE COOLED CAVITY OF PIV WITH COLORED SEEDING PARTICLES.

4. Spatial temperature and velocity field

4.1 Temperature distribution

Figure 5 shows the temperature distribution in the side-cooled cavity captured by dual-luminescence imaging. 100 images (1-sec period) were averaged to minimize the shot noise of the camera. The three thermocouples, which were used for temperature monitoring, are covered by black color in this figure. Cooled Toluene is seen along the cooled side and at the bottom of the cavity. The upper area is at a higher temperature marked by warmer colors. The colder temperature near the bottom was around zero degree Celsius. Three thermocouples monitored the temperature of the cooled Toluene. The monitored temperature by thermocouples were 9.5, 14.3, and 18.3 degrees Celsius from the bottom to the top. Those temperatures matched with the temperature that was captured by the dual-luminescence imaging. Some spots indicated colder areas, where are highlighted by circles, which are caused by coagulated particles in Toluene. The coagulated particles were excited by the light sources and emitted blue wavelength. Hence, even image rationing could not cancel out measurement errors as a geometric factor. This measurement error will be vanished by careful mixing of the seeding particle.

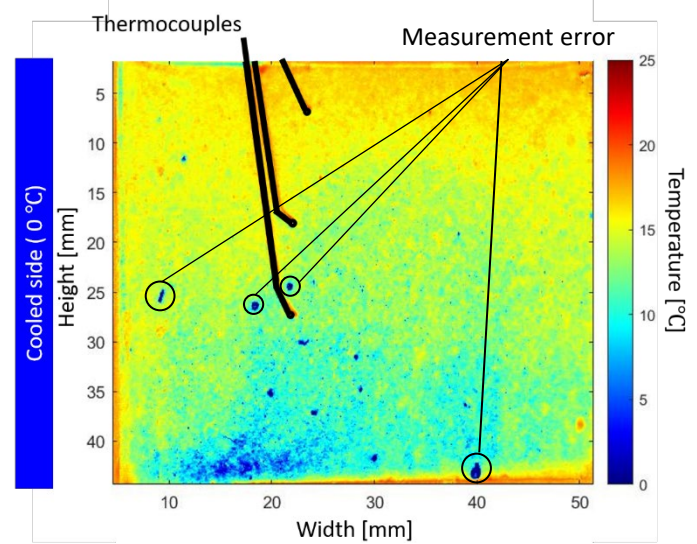


FIGURE 5: TIME-AVERAGED TEMPERATURE DISTRIBUTION OF THE SIDE COOLED CAVITY CAPTURED BY DUAL-LUMINESCENCE IMAGING

4.2 Velocity field

In this work, a GUI-based open-source tool (PIVlab) for PIV analyses in MATLAB was utilized [13]. The tool takes advantage of several built-in MATLAB features and eases subsequent data processing by providing a close link to the popular MATLAB user interface. Figure 6 shows the velocity magnitude field over the side-cooled cavity calculated by the PIV method. Higher velocity vectors can be seen near the cooled side of the cavity. This higher velocity field is derived by the

temperature difference between the oil and the cooled side. This temperature difference induced large circulation in the cavity. Figure 7 shows the raw image used for the PIV analysis. The red square indicates the area where fewer seeding particles are distributed. The cooled side area was expected to have a higher velocity toward the cavity bottom. However, this velocity field could not be observed due to the fewer particles. This area is one of the important areas to investigate the heat transfer pathway from the cooled side and the adjacent oil. Therefore, more particles need to be added to improve the measurement accuracy over this interesting area. Also, the camera setup should magnify this area to improve spatial resolution for future work.

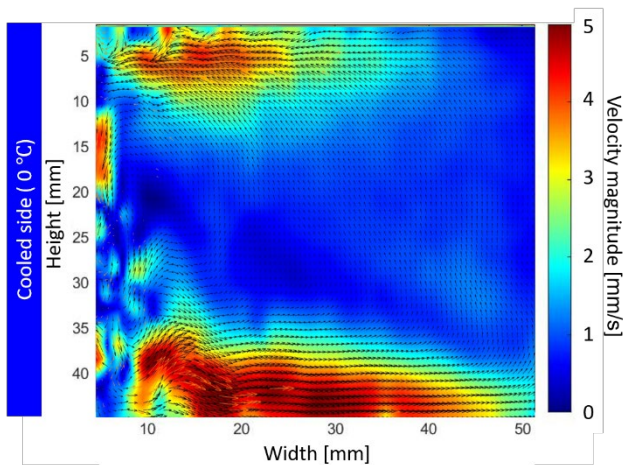


FIGURE 6: VELOCITY VECTORS AND MAGNITUDE FIELD OF THE SIDE COOLED CAVITY CAPTURED BY PARTICLE-BASED VELOCIMETRY

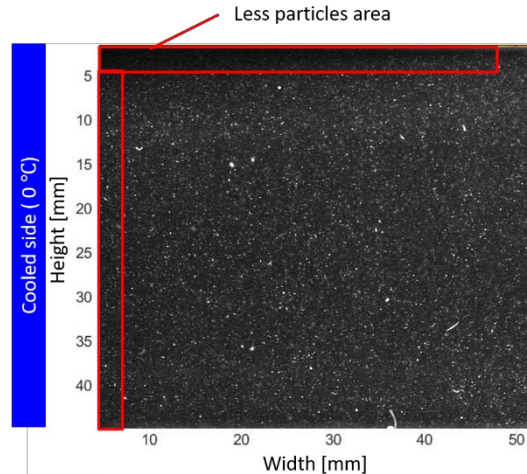


FIGURE 7: SINGLE RAW IMAGE OF THE SIDE COOLED CAVITY CAPTURED BY PARTICLE-BASED VELOCIMETRY METHOD.

5. CONCLUSION

A new simultaneous temperature and velocity measurement technique was developed by combining dual-luminescence imaging and particle-based velocimetry. Toluene, which imitates the spilled oil over the ice sea, dissolves two luminescent probes

for dual-luminescence imaging. One of the two luminescent probes is temperature-sensitive, and another one is temperature-insensitive. Fluorescein colored seeding particles to allow the green channel of the color camera to capture the luminescent intensity of the colored particles. As the first step of this work, two measurements were conducted separately. In the future, two measurements will be conducted simultaneously. The developed measurement system simultaneously extracted 2-D temperature and velocity field over the side cooled cavity. That extracted information will be substantial to analyze the heat transfer pathway in a liquid fuel adjacent to ice, resulting from the ice-melting acceleration. The side-cooled cavity simply imitated the ice-oil interface without dynamic motion due to the ice melting. As the final goal of this measurement method, development, simultaneous measurement under the ice-melting condition will be conducted.

ACKNOWLEDGEMENTS

This material is based upon work supported by the National Science Foundation under Grant No. 1938980. Any opinions, findings and conclusions or recommendations expressed in this material are those of the author(s) and do not necessarily reflect those of the National Science Foundation.

REFERENCES

- [1] D.S. Etkin, Analysis of oil spill trends in the united states and worldwide, 2005 Int. Oil Spill Conf. IOSC 2005. (2005) 293–302. <https://doi.org/10.7901/2169-3358-2001-2-1291>.
- [2] E. Arzaghi, R. Abbassi, V. Garaniya, J. Binns, F. Khan, An ecological risk assessment model for Arctic oil spills from a subsea pipeline, *Mar. Pollut. Bull.* 135 (2018) 1117–1127. <https://doi.org/10.1016/j.marpolbul.2018.08.030>.
- [3] T. Nordam, D.A.E. Dunnebie, C. Beegle-Krause, M. Reed, D. Slagstad, Impact of climate change and seasonal trends on the fate of Arctic oil spills, *Ambio*. 46 (2017) 442–452. <https://doi.org/10.1007/s13280-017-0961-3>.
- [4] H. Farmahini Farahani, G. Jomaas, A.S. Rangwala, Effects of convective motion in n-octane pool fires in an ice cavity, *Combust. Flame*. 162 (2015) 4643–4648. <https://doi.org/10.1016/j.combustflame.2015.09.021>.
- [5] H.F. Farahani, W.U.R. Alva, A.S. Rangwala, G. Jomaas, Convection-driven melting in an n-octane pool fire bounded by an ice wall, *Combust. Flame*. 179 (2017) 219–227. <https://doi.org/10.1016/j.combustflame.2017.02.006>.
- [6] H. Farmahini Farahani, Y. Fu, G. Jomaas, A.S. Rangwala, Convection-driven cavity formation in ice adjacent to externally heated flammable and non-flammable liquids, *Cold Reg. Sci. Technol.* 154 (2018) 54–62. <https://doi.org/10.1016/j.coldregions.2018.06.010>.
- [7] M. Tanaka, S. Kimura, K. Morita, H. Sakaue, Development and application of dual-luminescence

- imaging for capturing supercooled-water droplet under icing conditions, 5th AIAA Atmos. Sp. Environ. Conf. (2013) 1–7. <https://doi.org/10.2514/6.2013-2548>.
- [8] M. Tanaka, S. Kimura, K. Morita, H. Sakaue, Time-resolved temperature distribution of icing process of supercooled water in microscopic scale, *Trans. Japanese Soc. Med. Biol. Eng.* 51 (2013) 1–9. <https://doi.org/10.2514/6.2014-2329>.
- [9] Y. Egami, U. Fey, C. Klein, J. Quest, V. Ondrus, U. Beifuss, Development of new two-component temperature-sensitive paint (TSP) for cryogenic testing, *Meas. Sci. Technol.* 23 (2012). <https://doi.org/10.1088/0957-0233/23/11/115301>.
- [10] M.A. Northrup, T.J. Kulp, S.M. Angel, Fluorescent particle image velocimetry: application to flow measurement in refractive index-matched porous media, *Appl. Opt.* 30 (1991) 3034. <https://doi.org/10.1364/ao.30.003034>.
- [11] F. Pedocchi, J.E. Martin, M.H. García, Inexpensive fluorescent particles for large-scale experiments using particle image velocimetry, *Exp. Fluids*. 45 (2008) 183. <https://doi.org/10.1007/s00348-008-0516-2>.
- [12] B.J. Petrosky, P. Maisto, K. Todd Lowe, M.A. André, P.M. Bardet, P.I. Tiemsin, C.J. Wohl, P.M. Danehy, Particle image velocimetry applications using fluorescent dye-doped particles, 53rd AIAA Aerosp. Sci. Meet. (2015) 1–8. <https://doi.org/10.2514/6.2015-1223>.
- [13] W. Thielicke, E.J. Stamhuis, PIVlab – Towards User-friendly, Affordable and Accurate Digital Particle Image Velocimetry in MATLAB, *J. Open Res. Softw.* 2 (2014). <https://doi.org/10.5334/jors.bl>.